AIP | Journal of Applied Physics

Spin-glass freezing of maghemite nanoparticles prepared by microwave plasma synthesis

K. Nadeem, H. Krenn, T. Traussnig, R. Würschum, D. V. Szabó et al.

Citation: J. Appl. Phys. **111**, 113911 (2012); doi: 10.1063/1.4724348
View online: http://dx.doi.org/10.1063/1.4724348
View Table of Contents: http://jap.aip.org/resource/1/JAPIAU/v111/i11
Published by the American Institute of Physics.

Spin-glass freezing of maghemite nanoparticles prepared by microwave plasma synthesis

K. Nadeem,[1,2,a)] H. Krenn,[2] T. Traussnig,[3] R. Würschum,[3] D. V. Szabó,[4] and I. Letofsky-Papst[5]
[1]*Department of Physics, International Islamic University, Islamabad, Pakistan*
[2]*Institute of Physics, Karl-Franzens University Graz, Universitätsplatz 5, A-8010 Graz, Austria*
[3]*Institute of Materials Physics, University of Technology Graz, A-8010 Graz, Austria*
[4]*Institute for Advanced Materials—Materials Process Technology, Karlsruhe Institute of Technology (KIT), 76021 Karlsruhe, Germany*
[5]*Institute for Electron Microscopy, University of Technology Graz, Steyrergasse 17, A-8010 Graz, Austria*

(Received 16 March 2012; accepted 2 May 2012; published online 5 June 2012)

Magnetic properties of 6 nm maghemite nanoparticles (prepared by microwave plasma synthesis) have been studied by ac and dc magnetic measurements. Structural characterization includes x-ray diffraction and transmission electron microscopy. The temperature scans of zero field cooled/field cooled (ZFC/FC) magnetization measurements show a maximum at 75 K. The ZFC/FC data are fitted to the Brown-Néel relaxation model using uniaxial anisotropy and a log-normal size-distribution function to figure out the effective anisotropy constant K_{eff}. K_{eff} turns out to be larger than the anisotropy constant of bulk maghemite. Fitting of the ac susceptibility to an activated relaxation process according to the Arrhenius law provides unphysical values of the spin-flip time and activation energy. A power-law scaling shows a satisfactory fit to the ac susceptibility data and the dynamic critical exponent ($zv \approx 10$) takes value between 4 and 12 which is typical for the spin-glass systems. The temperature dependence of coercivity and exchange bias shows a sharp increase toward low temperatures which is due to enhanced surface anisotropy. The source of this enhanced magnetic anisotropy comes from the disordered surface spins which get frozen at low temperatures. Memory effects and thermoremanent magnetization experiments also support the existence of spin-glass behaviour. All these magnetic measurements signify either magnetic blocking or surface spin-glass freezing at high and low temperatures, respectively. © *2012 American Institute of Physics*. [http://dx.doi.org/10.1063/1.4724348]

I. INTRODUCTION

Nanoparticle magnetism is one of the most interesting fields in magnetism due to its dramatic changes as compared to bulk magnetism.[1–3] Spinel ferrite nanoparticles exhibit a variety of magnetic phases due to symmetry breaking and competing exchange interactions on the nanoparticle surface.[4,5] Kodama *et al.* have proposed a model of surface spin-glass freezing in nickel ferrite nanoparticles due to disorder and broken bonds with a concomitant reduction of saturation magnetic moment.[6,7] The influence of this disordered surface layer increases with decreasing particle size taking into account a shell/core morphology of irregularly frozen spins in the glassy shell and of collectively ordered spins in crystalline core.[8,9]

Maghemite (γ-Fe_2O_3) nanoparticles have been investigated intensively over the last years due to their potential applications in biomedical diagnostics and therapy, magnetic data recording and ferrofluids.[10–15] γ-Fe_2O_3 is one of the ferrimagnetic materials ordered with inverse spinel structure, but with vacancies at the octahedral sites. In spinel ferrite structure, oxygen forms a face-centered-cubic (FCC)-lattice with cations distributed over tetrahedral (A) and octahedral (B) sites. The unit cell of a spinel ferrite consists of 32 oxygen, 16 trivalent iron, and 8 divalent transition metal ions like nickel ($NiFe_2O_4$) or cobalt ($CoFe_2O_4$). Due to vacancies and competing interactions among spins located on different sublattices together with broken bonds, surface spins of maghemite nanoparticles experience frustration and disorder.[16] As the particle size is reduced, disorder and frustration at the nanoparticle's surface becomes progressively dominant with a tendency to form a spin-glass phase.[17,18] Winkler *et al.*[8] have reported spin-glass behavior in nickel oxide (NiO) nanoparticles, Peddis *et al.*[9] in fine cobalt ferrite ($CoFe_2O_4$) nanoparticles and attributed the spin-glass phase to a random freezing of surface spins. There are some theoretical models to separate blocking and surface spin-glass behaviour in nanoparticles but it is not easy to prove it experimentally. In this article, we will study the blocking state and ordering of the disordered surface spins of fine maghemite nanoparticles by analyzing dc and ac magnetic measurements.

II. EXPERIMENT

Fine maghemite nanoparticles have been prepared by microwave plasma synthesis using a 2.45 GHz microwave equipment and $Fe(CO)_5$ as precursor material. The complete synthesis process is described in detail in Ref. 19 and structural evaluation of the materials (made by the same synthesis process) is reported elsewhere.[20] Spinel structural phase was identified by x-ray diffraction (XRD) (Bruker D8 Advance

a)Author to whom correspondence should be addressed. Electronic addresses: kashif.nadeem@iiu.edu.pk and kashifnaddem@yahoo.com.

instrument) using Cu-K_α ($\lambda = 0.154$ nm) radiation at ambient conditions. Average particle size (6 nm) was evaluated by Debye-Scherrer's formula and compared with size-distribution statistics taken from an image analysis of transmission electron micrographs (TEM, model number CM20 from FEI with 200 kV acceleration voltage and LaB_6 cathode). Magnetic measurements were taken by using superconducting quantum interference device (SQUID)-magnetometry (Quantum Design, MPMS-XL-7) with maximum applied field of ± 7 T in the temperature range 4.2–300 K. The ac susceptibility measurements were performed by the same magnetometer in the frequency range 0.1–1000 Hz and in the temperature range 4.2–300 K. Due to the narrow size-distribution, our prepared maghemite nanoparticles are good model substances for a reliable distinction between freezing and magnetic blocking which is proved by simulations.

III. RESULTS AND DISCUSSION

Figure 1 shows the XRD diffraction pattern of maghemite nanoparticles. Debye-Scherrer's formula yields the average particle size of 6 nm. Figures 2(a) and 2(b) show the TEM images of maghemite nanoparticles with a magnification given by the scale of (a) 10 nm and (b) 2 nm, respectively. Inset of Fig. 2(a) shows the particle size distribution fitted with log-normal distribution. Average particle size calculated from such a fit is 6.1 nm with a normalized standard deviation $\sigma_D = 0.22$ which is in agreement with the XRD analysis. Figure 2(b) shows the TEM image at 2 nm scale which indicates that the particles are of crystalline form.

Now we will discuss the magnetic properties of these maghemite nanoparticles in detail. Figure 3 shows the zero field cooled hysteresis loops of maghemite nanoparticles at 300 and 4.2 K up to a maximum applied field of ± 5 T. Coercivity (H_c) comes out to be 11 and 546 Oe at 300 and 4.2 K, respectively. At low temperature frozen surface spins are pinned on the individual nanoparticle's surface and experience strong interactions with core spins. This effect causes a large increase of coercivity (H_c) at low temperature $T = 4.2$ K.[16]

Saturation magnetization (M_s) is found to be 42 and 51 emu/g at 300 and 4.2 K, respectively. The values of saturation magnetization at both temperatures are less than the saturation magnetization of bulk maghemite (M_s (bulk) = 80 emu/g), which is typical for maghemite nanoparticles due to spin-canting of surface spins. The increase of saturation magnetization (M_s) at low

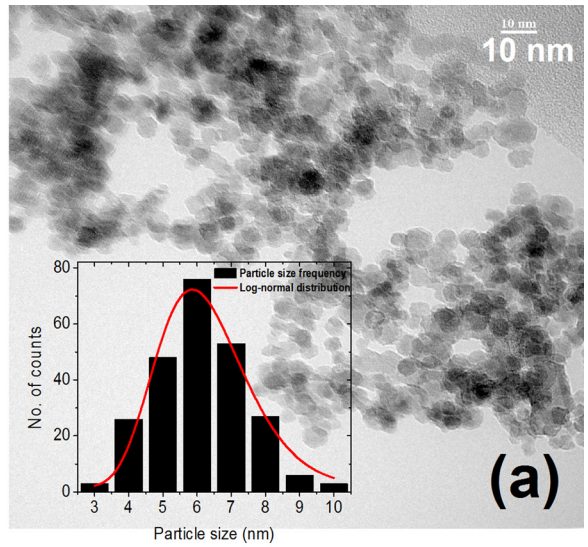

FIG. 2. TEM image of maghemite nanoparticles at (a) 10 nm and (b) 2 nm magnification scale, respectively. Inset in (a) shows the particle size distribution fitted with log-normal distribution.

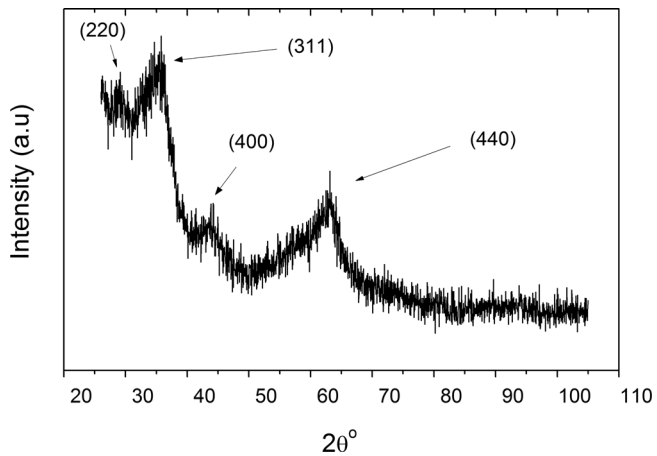

FIG. 1. X-ray diffraction spectra of maghemite nanoparticles.

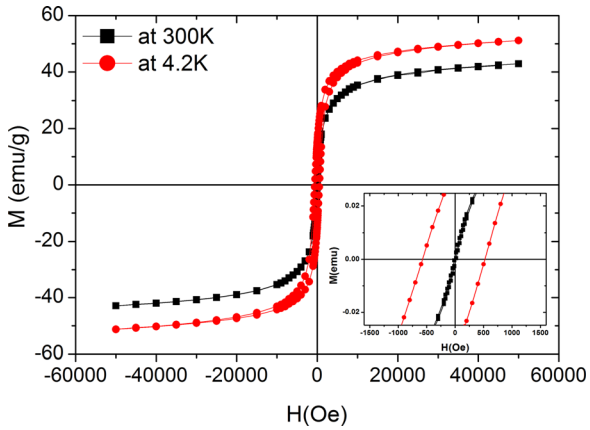

FIG. 3. Hysteresis loops of maghemite nanoparticles at temperature T = 300 and 4.2 K.

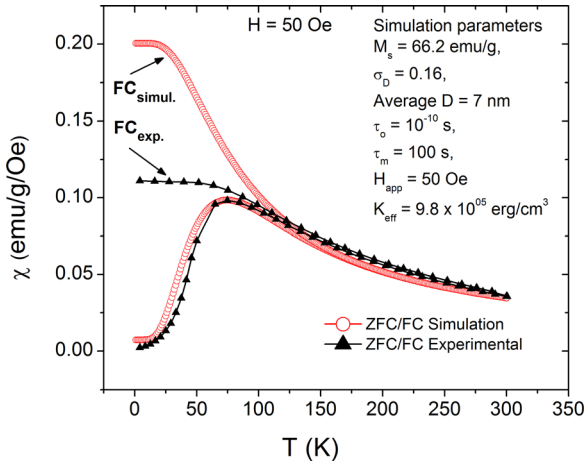

FIG. 4. Solid triangles: Experimental ZFC/FC susceptibility curves under applied field of 50 Oe of maghemite nanoparticles. Hollow circles are simulations of ZFC and FC curves, respectively, under field H = 50 Oe using Eqs. (3) and (4). Simulation parameters are listed in the figure.

temperature 4.2 K is due to a decrease of thermal fluctuations of magnetic moments on the surface.[6,7]

Figure 4 shows the experimental (solid triangles) and simulated (hollow circles) zero field cooled/field cooled (ZFC/FC) magnetization curves under applied field of 50 Oe of maghemite nanoparticles. For ZFC/FC experimental measurements, first the sample is cooled in zero field from room temperature to 4.2 K. Thereafter 50 Oe magnetic field is applied and magnetic moment is recorded with increasing temperature to get the ZFC curve. For the FC curve, the sample is cooled from 300 K under the same 50 Oe field and magnetic moment is recorded on decreasing temperature. The ZFC curve reveals a maximum at temperature T = 75 K which is the average blocking temperature (T_B) of these maghemite nanoparticles.

We have also compared our ZFC/FC experimental results with the theory.[21,22] For simulation, we have used the Néel-Brown relaxation model adopting uniaxial anisotropy. The assumed log-normal distribution function of particle sizes is reproduced by a corresponding log-normal distribution function of blocking temperatures T_B,

$$f(T_B)dT_B = \frac{1}{\sqrt{2\pi\sigma_{TB}^2}}\frac{1}{T_B}\exp\left(-\frac{\ln^2\frac{T_B}{\langle T_B\rangle}}{2\sigma_{TB}^2}\right)dT_B. \quad (1)$$

This is acceptable since the average blocking temperature $\langle T_B\rangle$ scales with the average particle volume $\langle V\rangle = \pi\langle d\rangle^3/6$. The quasi-static ZFC/FC- magnetization scans measured by a SQUID magnetometer rely on a characteristic measurement time $\tau_m \approx 100$ s in relation with the atomic spin precession time $\tau_0 \approx 10^{-10}$ s,

$$\langle T_B\rangle = \frac{K_{eff}}{k_B \ln\left(\frac{\tau_m}{\tau_0}\right)}\langle V\rangle. \quad (2)$$

According to the model for non-interacting particles, the ZFC susceptibility is given by[23]

$$\chi_{ZFC}(T) = \frac{M_s^2}{3K_{eff}}\left[\ln\left(\frac{\tau_m}{\tau_o}\right)\int_0^T \frac{T_B}{T}f(T_B)dT_B + \int_T^\infty f(T_B)dT_B\right]. \quad (3)$$

For a certain temperature T the first and second term in Eq. (3) correspond to de-blocked superparamagnetic and frozen blocked particles, respectively.

According to the same model, the FC susceptibility is given by[23]

$$\chi_{FC}(T) = \frac{M_s^2}{3K_{eff}}.\ln\left(\frac{\tau_m}{\tau_o}\right)\left[\frac{1}{T}\int_0^T T_B f(T_B)dT_B + \int_T^\infty f(T_B)dT_B\right]. \quad (4)$$

The best fit of the model to experimental ZFC/FC data yields $K_{eff} = 9.8 \times 10^{05}$ erg/cc and an average particle size $\langle d\rangle = 7$ nm. The increased value of fitted K_{eff} with respect to bulk maghemite $K_{Bulk} = 4.7 \times 10^4$ erg/cc (Ref. 5) arises from an additional surface anisotropy caused by random frozen surface spins.[7] There is a difference between the experimental and simulated FC curves. The difference comes because the model assumes only non-interacting single-domain particles. The experimental field cooled ($FC_{exp.}$) curve flats immediately below the blocking peak but the simulated FC curve ($FC_{simul.}$) continues to increase and flattens at much lower temperatures. The flattening of the $FC_{exp.}$ curve just below the blocking peak is an indication of the presence of interparticle and/or surface spin-glass freezing in these nanoparticles.[16–18]

To investigate in detail the spin-glass behaviour, we have measured the frequency dependence of ac susceptibility. For ac susceptibility measurements, first the sample is cooled from room temperature to 4.2 K in zero applied field and then ac susceptibility is measured with increasing temperature. Figure 5(a) shows the frequency dependence of in-phase ac susceptibility of maghemite nanoparticles in the frequency range 0.1–1000 Hz and for ac signal amplitude A = 5 Oe.

The ac susceptibility scales with frequency according to Eq. (5) by replacing $\tau_m \rightarrow 1/\omega$, with a maximum at a frequency dependent blocking temperature $\langle T_B\rangle \approx T_S$ which shifts towards higher temperature with increasing frequency. Arrhenius law is fitted to the temperature dependence of the ac susceptibility peak and presented in the *inset* of Fig. 5(b). Arrhenius law is defined as

$$\tau = 1/\omega_p = \tau_o.\exp\left(\frac{E_a}{k_B T_s}\right), \quad (5)$$

where τ_o is the atomic spin flip time, $E_a = K_{eff}V$ is the activation energy, T_s is the peak temperature, and k_B is the Boltzmann constant. It gives unreasonable values for spin-flip time $\tau_o = 3 \times 10^{-18}$ s and for the activation energy (in Kelvin units) $E_a/k_B = 3637$ K. These wrong findings indicate that the maximum of ZFC and ac susceptibility does not correspond to only a thermally activated process.

Dynamic scaling law is usually applied to investigate spin-glass systems. The frequency shift is also fitted to a dynamic scaling law as defined in Ref. 24 and shown in Fig. 5(b),

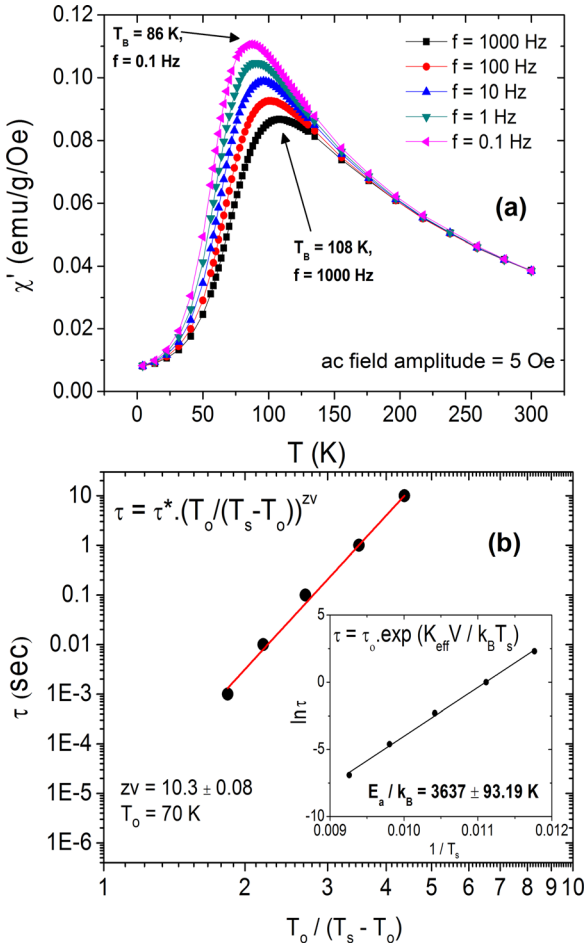

FIG. 5. (a) Frequency dependence of in-phase ac susceptibility of maghemite nanoparticles, (b) fitting of the dynamic scaling law (Eq. (6)) to the frequency dependent ac susceptibility of maghemite nanoparticles. Inset shows the (unphysical) fitting by Arrhenius law (Eq. (5)).

$$\tau(f) = \tau^* \cdot \left[\frac{T_o}{T_s(f) - T_o}\right]^{zv}. \qquad (6)$$

In Eq. (6), τ(f) is the frequency dependent relaxation time of frozen spins, τ^* is related to the coherence time of coupled individual spins in the nanoparticle, T_o is the "static" ($f \to 0$) spin-glass freezing temperature, "zv" the critical exponent (ranging from 4–12 for different spin-glass systems[25,26]), and T_s(f) is the frequency dependent freezing temperature as given by the maxima of the χ'(T)-plots (see Fig. 5(a)). Scaling law indicates that there is a critical slowing down of relaxation time near the spin-glass transition temperature T_o. We have taken T_s(f) as the maximum of ac susceptibility curve. The result of the fit is shown in Fig. 5(b). It yields the transition temperature $T_o = 70$ K which is in good agreement with the blocking temperature peak (T_B) of the dc measurements (see Fig. 4). The fitted spin flip time is $\tau^* \approx 10^{-06}$ s and $zv \approx 10$. The increased value of spin flip time τ^* is due to frozen agglomerates of highly disordered and frustrated surface spins which have a much longer relaxation time than the individual spins. The fitted critical exponent ($zv \approx 10$) falls in the spin-glass regime which indicates the existence of spin-glass freezing in these maghemite nanoparticles. The origin of spin-glass freezing in uncoated fine nanoparticles is the random freezing of disordered and frustrated spins at the surface of individual nanoparticles.[5,16,27]

Temperature dependent hysteresis parameters (especially coercivity) provide additional information about the frozen surface spins and their interactions with the core spins. Figure 6 shows the temperature dependent coercivity (H_c) and the exchange bias field ($H_{exc.}$) of maghemite nanoparticles. Coercivity (H_c) is vanishing in the temperature range 75–300 K due to superparamagnetic de-blocking behaviour which is in agreement with the ZFC/FC measurements (see Fig. 4). Collapse of coercivity (H_c) is interpreted as thermal de-blocking of the giant core spin above the blocking temperature $T_B = 75$ K. Therefore in the zero coercivity region, the nanoparticles behave superparamagnetic and the core spin of every nanoparticle can easily follow the external magnetic field.[28] Below the blocking temperature ($T < 75$ K), coercivity (H_c) shows a sharp increase (up to 538 Oe) with decreasing temperature. This sharp increase is again due to the enhanced surface anisotropy (in accordance with simulation results) and pinning effects at the nanoparticle's surface which causes hindrances for the core spin to follow the external magnetic field.

Freezing of surface spins by cooling in zero field causes an exchange bias effect (represented by the exchange bias field $H_{exc.}$) which is manifested by a horizontal shift of the hysteresis loop upon field cooling of nanoparticles.[29,30] The exchange bias field ($H_{exc.}$) experiences a sharp increase at low temperature and vanishes above 30 K as shown in Fig. 6. The inset shows a detail of the hysteresis of maghemite nanoparticles after ZFC and FC (@ 5 T) at temperature $T = 4.2$ K near the coercive field in magnified view. It verifies the exchange bias ($H_{exc.}$) effect in these nanoparticles. The increased core-shell interactions are responsible for the sharp increase of the exchange bias field at low temperatures. As the temperature increases, the core-shell interaction becomes quenched above 30 K due to start of de-blocking of surface spins. Martínez *et al.*[16] also reported a sharp increase of exchange bias and coercivity at low temperatures in maghemite nanoparticles. The presence of exchange bias and sharp increase in coercivity at low temperatures indicates that the spin-glass freezing

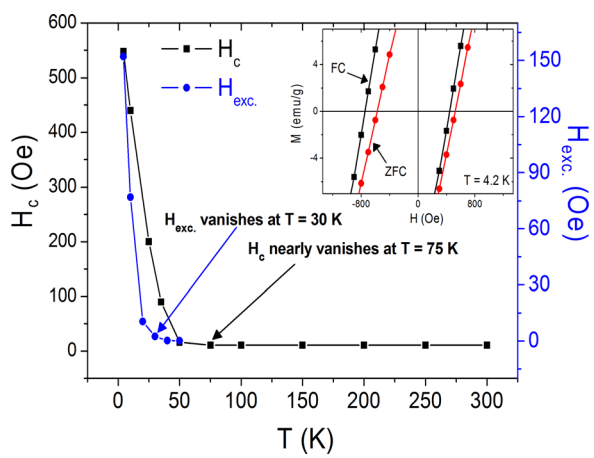

FIG. 6. Temperature dependence of coercivity (H_c) and exchange bias field ($H_{exc.}$) of maghemite nanoparticles. Inset: Coercivity region of hysteresis loops after ZFC and FC (5 T) at 4.2 K, respectively. Note the asymmetric horizontal shift of FC hysteresis loop due to the exchange bias effect.

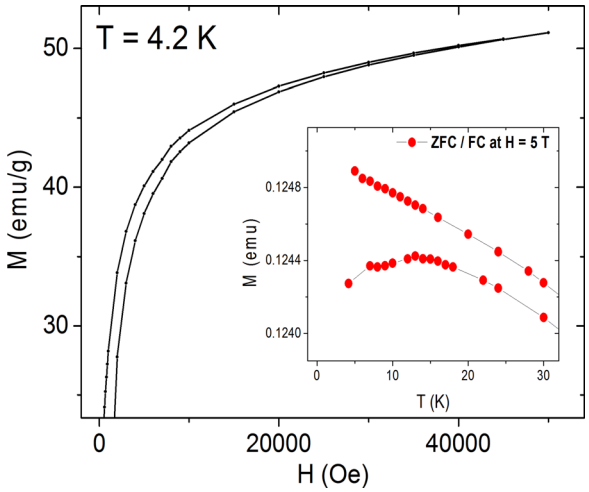

FIG. 7. Upper branch of the hysteresis loop of maghemite nanoparticles at temperature T = 4.2 K. Inset: Low temperature region of the splitted ZFC/FC magnetization under applied field H = 5 T.

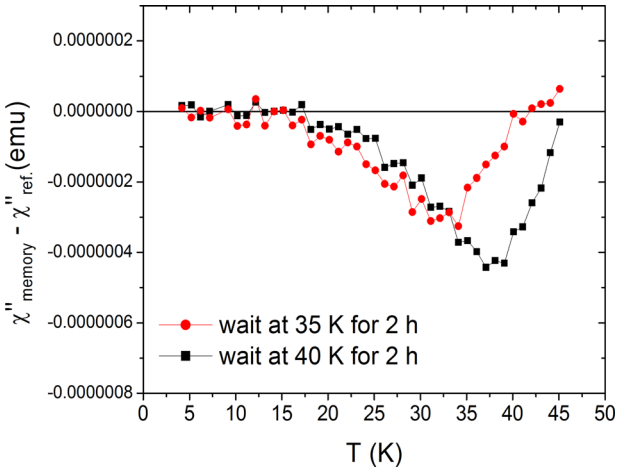

FIG. 8. Difference of out-of-phase ac susceptibility memory curve (when the system is halted at 35 and 40 K for 2 h) and the respective reference curves of maghemite nanoparticles.

(as indicated by fitting of scaling law) comes from the random freezing of surface spins on the individual nanoparticle surface.

High field irreversible magnetic behaviour of nanoparticles and an opening of hysteresis loop up to the high fields accounts for an enhanced surface anisotropy. Figure 7 shows the positive branch of the hysteresis loop at 4.2 K and *inset* shows the low temperature region of ZFC/FC magnetization under applied field of 5 T for maghemite nanoparticles.

The zero field cooled hysteresis loop at 4.2 K is irreversible up to a field of 5 T which is caused by frozen surface spins at low temperatures. Inset shows the low temperature region of the ZFC/FC magnetization under high field H = 5 T. ZFC and FC branches are open even at the highest field 5 T. Again, this irreversible behavior is due to the addressed surface effects and in agreement with the simulation results as already discussed.

We have also checked existence of memory effects in our sample, which are more unique *fingerprints* of spin-glass behavior.[31,32] In the memory experiment, a measuring protocol at two temperature scans is performed, one is the reference curve and the other is memory curve (for which the system is halted below spin-glass temperature for a specified time). To get the reference curve, sample is zero field cooled from room temperature to 4.2 K in zero applied field and then out-of-phase ac susceptibility is recorded immediately on increasing temperature. For the memory curve, the sample is also zero field cooled to a certain waiting temperature (in our case 35 and 40 K) and halted there for some specific time (in our case 2 h). After this, the cooling is continued to 4.2 K and then out-of-phase ac susceptibility is recorded on increasing temperature.[32,33] Here we have measured the out-of-phase ac susceptibility because it is directly related to the corresponding relaxation losses in the sample. Any difference between the reference and memory curve indicates the presence of a memory effect in the sample. Figure 8 shows the difference of out-of-phase ac susceptibility (f = 10 Hz, A = 5 Oe) memory curve (when the system is halted at 35 and 40 K for 2 h) with respect to the reference curve.

The difference between the corresponding memory and reference curve shows a dip near the waiting temperatures (35 and 40 K), which demonstrates the existence of memory effect of the system onto the earlier stop at the corresponding waiting temperature. Bisht and Rajeev[34] have reported memory and aging effects in fine 5 nm NiO nanoparticles and attributed them to spin-glass freezing at the nanoparticle's surface at low temperatures. In the memory curve, magnetic moment decreases near the waiting temperature because the system remembers of its (originally disordered) magnetic state at the waiting temperature. The waiting temperatures (35 and 40 K) have been chosen below the onset of spin-glass freezing and below the turn-on of the coercivity enhancement temperatures (see Fig. 6). At these temperatures, disorder among surface spins develops due to an increase of the spin-glass correlation length on the surface of the particles.

Since the early days of spin-glass research, thermoremanent magnetization (TRM) has been discovered as a selective method to study the magnetic relaxation in spin-glasses. We have used relaxation of the thermoremanent magnetization at different temperatures to study the relaxation of core and surface spins.[31,33,35] Figure 9 shows the time dependent TRM of maghemite nanoparticles at different temperatures. For these measurements, the sample is field cooled in 50 Oe from room temperature to the measuring temperature (20–150 K) and thereafter field is switched off and the magnetic moment is recorded as a function of time.

At 20 K, both surface and core spins are frozen along random directions and become blocked along their anisotropy axes. There is slow-down of magnetization relaxation with increasing time upon removal of external magnetic field. The slope of the TRM curve changes near the spin-glass as well as at the blocking temperature as indicated by rectangles in Fig. 9. First in the 30–40 K temperature region, the TRM curve changes with the quench of core-shell interactions which is consistent with the vanishing exchange bias field ($H_{exc.}$) in the same temperature region (see Fig. 6). Near the blocking temperature ($T_B = 75$ K), the surface spins are already de-blocked from their anisotropy axes, therefore the change of the slope of TRM curve at this temperature originates from the de-blocking of the individual nanoparticle's gaint core spin and is also in agreement with the vanishing coercivity (H_c) above the blocking temperature (see Fig. 6).

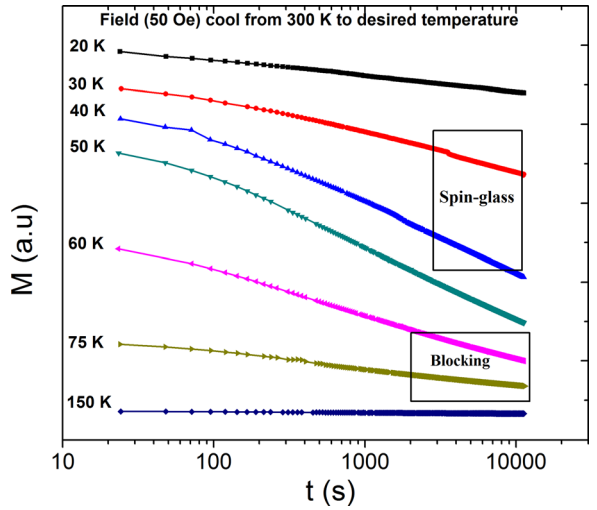

FIG. 9. Relaxation of the TRM of maghemite nanoparticles at different temperatures (in the range 20–150 K).

IV. CONCLUSION

In this study, maghemite nanoparticles have been prepared by microwave plasma synthesis which avoids agglomeration of particles due to charging in the plasma. The magnetic properties are investigated in detail. ZFC measurements show a well-defined blocking temperature at $T = 75$ K which indicates the narrow particle size distribution as it is evidenced by TEM analysis and in good agreement with ZFC/FC simulations. The simulated dc FC susceptibility curve flattens at a much lower temperature than in the experiment ($T_B = 75$ K) which indicates the presence of an additional cooperative phenomenon which is interpreted as a spin-glass state in contrast to interparticle interactions. Fitting of ZFC/FC curves yields an increased value of the effective anisotropy constant (K_{eff}) with respect to bulk maghemite. The frozen surface spins act as pinning centers on the surface and modifies the exchange interaction with the core spins (exchange bias). Freezing also mediates an additional contribution to the on-site magnetocrystalline anisotropy of the core spins. Simulations also show a discrepancy of the $FC_{simul.}$ susceptibility scan with the experimental $FC_{exp.}$ It is attributed to the surface spin-glass state and rules out interparticle (dipolar) interactions, since the temperature of the observed features is relatively high (35–40 K). Arrhenius law does not fit frequency dependent ac susceptibility. Such an attempt gives unphysical values of spin-flip time (τ_o) and activation energy (E_a) in contrast to a successful fit to a dynamic scaling law with a critical dynamic exponent $z\nu \approx 10$.

Exchange bias ($H_{exc.}$) shows a sharp increase at low temperature due to turn-on core-shell interactions. Disorder and frustration on the surface of the nanoparticles prevents nucleation of groups of reversed spins at the core-shell-interface which is manifested by the sharp increase of coercivity at low temperatures. A direct proof of spin-glass effects is given by the observation of memory effects in zero field cooling. Relaxation of the TRM is reflected by a change of the magnetic viscosity (the slope of TRM curves) near the spin-glass and blocking temperatures, respectively. In conclusion, microwave plasma-deposited maghemite nanoparticles are good archetypes for an investigation of cooperative magnetic phenomena beyond the conventional magnetic blocking effect.

ACKNOWLEDGMENTS

K. Nadeem acknowledges the Higher Education Commission (HEC) of Pakistan for providing research funds. The authors also thank the Austrian Science Fund (FWF) (national funds) for granting the network projects (NFN) S10407-N16, S10405-N16, and the NAWI-Graz GASS cooperation project.

[1]S. Linderoth, P. V. Hendriksen, F. Bødker, S. Wells, K. Davis, S. W. Charles, and S. Mørup, J. Appl. Phys. **75**, 6583 (1994).
[2]S. Mørup, Europhys. Lett. **28**, 671 (1994).
[3]S. Middey, S. Jana, and S. Ray, J. Appl. Phys. **108**, 043918 (2010).
[4]*Surface Effects in Magnetic Nanoparticles*, 1st ed., edited by D. Fiorani (Springer, New York, 2005).
[5]D. Fiorani, A. M. Testa, F. Lucari, F. D'Orazio, and H. Romero, Physica B **320**, 122–126 (2002).
[6]R. H. Kodama and A. E. Berkowitz, Phys. Rev. B **59**, 6321 (1999).
[7]R. H. Kodama, A. E. Berkowitz, E. J. McNiff, and S. Foner, Phys. Rev. Lett. **77**, 394 (1996).
[8]E. Winkler, R. D. Zysler, M. Vasquez Mansilla, D. Fiorani, D. Rinaldi, M. Vasilakaki, and K. N. Trohidou, Nanotechnology **19**, 185702 (2008).
[9]D. Peddis, C. Cannas, G. Piccaluga, E. Agostinelli, and D. Fiorani, Nanotechnology **21**, 125705 (2010).
[10]R. M. Cornell and U. Schwertman, *The Iron Oxides, Structure, Properties, Reactions, Occurrences and Uses* (Wiley-VCH, Weinheim, 2003).
[11]M. Srivastava, A. K. Ojha, S. Chaubey, and A. Materny, J. Alloys Compd. **481**, 515 (2009).
[12]C. Sun, J. S. H. Lee, and M. Zhang, Adv. Drug Delivery Rev. **60**, 1252 (2008).
[13]L. Yang, Y. Xie, H. Zhao, X. Wu, and Y. Wang, Solid-State Electron. **49**, 1029 (2005).
[14]E. Hee Kim, H. Sook Lee, B. Kook Kwak, and B. Kim, J. Magn. Magn. Mater. **289**, 328 (2005).
[15]S. A. Wolf, D. D. Awschalom, R. A. Buhrman, J. M. Daughton, S. von Molnár, M. L. Roukes, A. Y. Chtchelkanova, and D. M. Treger, Science **294**, 1488 (2001).
[16]B. Martínez, X. Obradors, L. I. Balcells, A. Rouanet, and C. Monty, Phys. Rev. Lett. **80**, 181 (1998).
[17]D. Parker, V. Dupuis, F. Ladieu, J. P. Bouchaud, E. Dubois, R. Perzynski, and E. Vincent, Phys. Rev. B **77**, 104428 (2008).
[18]S. Nakamae, Y. Tahri, C. Thibierge, D. L. Hôte, E. Vincent, V. Dupuis, E. Dubois, and R. Perzynski, J. Appl. Phys. **105**, 07E318(2009).
[19]D. Vollath and D. V. Szabó, J. Nanopart. Res. **8**, 417–428 (2006).
[20]D. Vollath, D. V. Szabó, R. D. Taylor, and J. O. Willis, J. Mater. Res. **12**(8), 2175–2182 (1997).
[21]W. F. Brown, Phys. Rev. **130**, 1677 (1963).
[22]L. Neel, Ann. Geophys. (C.N.R.S.) **5**, 99 (1949).
[23]J. C. Denardin, A. L. Brandl, M. Knobel, P. Panissod, A. B. Pakhomov, H. Liu, and X. X. Zhang, Phys. Rev. B **65**, 064422 (2002).
[24]P. C. Hohenberg and B. I. Halperin, Rev. Mod. Phys. **49**, 435–479 (1977).
[25]J. A. Mydosh, *Spin Glasses* (Taylor & Francis, Washington, 1993).
[26]K. H. Fischer and J. A. Hertz, *Spin Glasses* (Cambridge University Press, Cambridge, 1991).
[27]G. C. Papaefthymiou, Nanotoday **4**, 438 (2009).
[28]C. N. Chinnasamy, A. Narayanasamy, N. Ponpandian, R. J. Joseyphus, B. Jeyadevan, K. Tohji, and K. Chattopadhyay, J. Magn. Magn. Mater. **238**, 281 (2002).
[29]J. Nogués, J. Sort, V. Langlais, V. Skumryev, S. Suriñach, J. S. Muñoz, and M. D. Baró, Phys. Rep. **422**, 65 (2005).
[30]M. Kiwi, J. Magn. Magn. Mater. **234**, 584 (2001).
[31]M. Sasaki, P. E. Jönsson, H. Takayama, and H. Mamiya, Phys. Rev. B **71**, 104405 (2005).
[32]K. Nadeem, H. Krenn, T. Traussing, and I. Letofsky-Papst, J. Appl. Phys. **109**, 013912 (2011).
[33]T. Jonsson, J. Mattsson, C. Djurberg, F. A. Khan, P. Nordblad, and P. Svedlindh, Phys. Rev. Lett. **75**, 4138 (1995).
[34]V. Bisht and K. P. Rajeev, J. Phys.: Condens. Matter **22**, 016003 (2010).
[35]P. Jönsson, M. F. Hansen, and P. Nordblad, Phys. Rev. B **61**, 1261 (2000).